Analytical Model for the Material Flow during Cold Rolling

János György Bátorfi[12*], Mátyás Andó[1], Jurij J. Sidor[1]

[1]Savaria Institute of Technology, Faculty of Informatics, Eötvös Loránd University, Károlyi Gáspár tér 4, H-9700 Szombathely, Hungary, bj@inf.elte.hu, am@inf.elte.hu, js@inf.elte.hu

[2]Doctoral School of Physics, Faculty of Natural Sciences, Eötvös Loránd University, Pázmány Péter sétány 1/A, H-1117 Budapest, Hungary, bj@inf.elte.hu

[*]Corresponding author, e-mail: bj@inf.elte.hu

Abstract: An analytical description of conventional cold rolling, is developed with a novel mathematical algorithm, based on finite element (FEM) and flow-line (FLM) method calculations. A new function, enabling the formulation of deformation, accurately describes the possible reverse displacement near the surface of a rolled sheet. The corresponding value of deformation can be determined for various friction coefficients and roll gap geometries by employing the expressions developed. Knowing the material flow, the amount of deformation and stress distribution along the thickness of the rolled sheet can be calculated. The results obtained were compared to the counterparts computed by FEM and FLM. It was shown that the extended model ensures accurate description of the material flow for small thickness reductions and low friction coefficients, where the phenomena of reverse displacement are observed, and many numerical approaches fail to capture this type of deformation pattern. The model was tested on both experimentally measured results and data obtained from various literature sources.

Keywords: Cold rolling; Symmetric rolling; Shear deformation; Reverse displacement; FEM; FLM

1 Introduction

Properties of the conventionally produced flat-rolled products are strongly affected by the following technological parameters: angular velocity and diameter of rolls, friction coefficient, yield stress of materials, reduction and deformation temperature. In view of the complexity of rolling process, the material flow is generally examined by experimental measurements [1] [2], finite element modeling (FEM) [3], flow-line models (FLM) [3-8] or other analytical methods [9] [10].

In most general case, the simplest approximation called plane strain compression (PSC) is employed which considers only the normal component of deformation, while the contribution of friction with corresponding shear components is neglected. Here, the amount of strain component in the thickness direction is approximated by the following expression, this component can be called the reduction too:

$$r = \frac{h_0 - h}{h_0} \tag{1}$$

where h_0 and h are initial and final thicknesses of a sheet subjected to rolling.

This simple approach does not account for accurate estimation of equivalent strain, rolling force and torque, whereas the reasonable estimate of the technological parameters can be done by FEM, where the properties of a material, friction conditions and parameters of a roll gap should be set. The well-established FEM models are based on the theory of plasticity with specified material parameters and can be used for simulating numerous mechanical problems. In the simulation, the material subjected to deformation is subdivided to numerous volume elements by a network of points whereas the stiffness equation system is imposed to specified boundary conditions, which define the displacement of a given group of points. Knowing the deformation of each element, both strains and stresses can be calculated, which makes possible the evaluation of these quantities in diverse planes and directions. Application of this numerical approach requires significant computational capacity. The calculation time depends on the material model used, boundary conditions imposed, type and size of mesh generated, and a number of steps defined. For instance, simulation of rolling process by employing a very fine mesh and nonlinear material model can take approximately 2 weeks or even longer, depending on the capacity of the personal computer used.

In contrast to FEM, flow line models (FLM) [3-8] offer fast and relatively accurate analytical solutions for specific deformation processes such as sheet rolling, bending or extrusion. Employing FLM approximations requires the definition of model parameters, which might be related to the boundary conditions of deformation process, however, in many instances, the fitting parameters do not reveal physical meaning, which complicates the implementation of this numerical approach in industrial practice. In case of rolling, FLMs engage streamlines which enforces the material to flow along these predefined directions with specific velocity, whereas the heterogeneity of strain/stress distribution is predefined by model parameters. For instance, in the model of Decroos et al. [7], the model parameters α and n ensures diverse deformation velocities along various streamlines and as it turned out both values are functions of friction coefficient and roll gap geometry and can be defined as it is described in Ref. [6]. In many instances, the FLM [7] ensures results comparable to FEM [5-8]. In addition to FLMs, alternative approximations [9, 10] provide accurate solutions exclusively for small values of friction coefficient.

It should be noted that the friction coefficient of Coulomb model (μ) is not constant in cold rolling, and the temperature of material changes either but the temperature variation has a negligible effect on material flow. In cold rolling of Al alloys, an increase of temperature in one deformation pass is far below one needed for recovery or recrystallization, however, the smallest changes in friction tend to induce strong strain/stress heterogeneities across the thickness of rolled sheet, which in turn has a strong influence on recrystallization phenomena during the subsequent annealing process. In this view, the determination of μ is of crucial importance. It is generally known that rolling is possible if μ exceeds the minimum value μ_{min} necessary for the process to be completed [11]:

$$\mu_{min} = \frac{1}{2}\sqrt{\frac{h}{R}}\frac{\ln\left(\frac{h_0}{h}\right)+\frac{1}{4}\sqrt{\frac{h_0-h}{R}}}{\tan^{-1}\sqrt{\frac{h_0}{h}-1}} \tag{2}$$

where R is a roll radius.

There are other literatures, such as the one described in [14], which also takes horizontal forces into account.

To evaluate the strain in rolling, Inoue [15] employs three basic assumptions: 1) the value of shear does not grow linearly; 2) the shear strain can decrease after reaching neutral point; 3) there is a plane strain state in the sheet and the normal strain is uniform through the thickness. Apart from mentioned approximation, there are many literature sources dealing with the strain heterogeneities which evolve in rolled materials across the thickness [5] [12] [13], however, there are still many issues which are not entirely understood or cannot be captured by numerical methods.

There are many other modelling methods, like the “Genetic Algorithm” based on “Artificial Neutral Network” [14].

In this contribution, we present a new mathematical formulation allowing fast and accurate estimation of strain/stress heterogeneities.

2 Computational Procedure

The evolution of strain in rolling was investigated by FEM simulations. Since cold rolling does not account for widening, the calculations were performed with Deform 2D© software. Cold rolling is a symmetric process and therefore, the boundary conditions are defined to the rolls and symmetry line. All simulations were carried out with the constant friction coefficient for the Coulomb model, the

value of which exceeds μ_{min}. This minimal value is changing between 0.015 and 0.05. The behavior of a material is described by the plastic-multilinear model with a constant Young's modulus of 68.9 GPa and Poison's ratio of 0.33. The plastic properties are the same as applied in [5] and as it is described later in Eq. (15). The mesh of a rolled sheet is divided into 50x11 elements, while half of the thickness is separated into 10 layers. In the calculation procedure, 59 different parameter set were used, and 11 points were taken along the half-thickness of the sheet, so the mathematical function introduced below was fitted to the results of 649 points. The amount of reduction on the material flow was analyzed by changing the degree of deformation and friction conditions. The applied geometrical values are the following: 250 mm is the radius of the roll, the velocity is 2 m/min, the initial half-thickness is 2 mm, the final thickness is changing between 0.6 and 0.9 mm, the friction coefficient is changing between 0.025 and 0.25.

3 New Mathematical Formulation of Rolling

As Fig. (1) shows, the material flow in rolling, revealing diverse patterns, is strongly correlated to the roll gap geometry. It is obvious that the distorted patterns of Fig. (1) can be successfully described by analytical approximations where the displacement is approximated by a quadratic function in the horizontal direction, Eq. (3). This function is capable of describing the experimental patterns as well [1]. Analyzing the experimentally observed [1] displacement of initially vertical line, it becomes clear that the stress/strain state during rolling can be considered as a plane strain one.

$$x = Az^2 \tag{3}$$

where x and z are parallel to rolling (x) and normal (z) directions, respectively, and A is a constant.

The precise description of deformation is important since it allows understanding the evolution of crystallographic texture in rolled materials [3-7]. Knowing the variations of texture evolved enables the evaluation of mechanical properties and their anisotropy.

In most general case, the distortion of the initially rectangular grid can be described by a simple analytical expression, Eq. (4). This type of displacement function is predicted by the flow line models, FEM and likewise observed experimentally [6] [7] [15]. It turns out that the model parameters α and n are functions of roll gap geometry and friction coefficient [6] [7].

$$x = \alpha z^n \tag{4}$$

It should be noted that mathematical expressions of Eqs. (3) and (4) describes the displacement fields with relatively good accuracy, however, a new exponential function Eq. (5) was introduced for more complex shaped curves, since the function presented by Eq. (4), is not capable of characterizing the phenomenon of reverse displacement, described in detail below. In some instances, [6] [16] [17], the maximal shear strain is localized in the subsurface layers and this phenomenon cannot be captured by a simple polynomial expression. Fig. (2) shows several examples of deformation patterns which can be reproduced by the extended function.

$$x = B_1(e^{-B_2 z^2} - 1) + B_3 z^2 \tag{5}$$

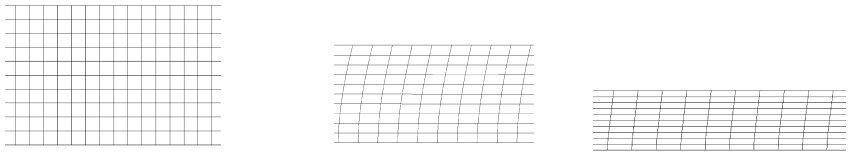

(a) (b) (c)

Figure 1

Distortion of mesh used in FEM simulations: a) initial mesh; b) mesh after 30% reduction with friction coefficient of 0.08; c) mesh after 50% reduction with friction coefficient of 0.08 (the initial thickness of Al sheet is 2 mm while the roll diameter is 250 mm; only the half-thickness is revealed due to symmetry imposed by rolling)

This complex equation is particularly advantageous in the cases when the reverse displacement occurs near the surface of the sheet leading to a strong deviation from the parabolic curve.

The shape of curve expressed by Eq. (5) can be controlled by varying the model parameters B_1, B_2 and B_3. As Fig. (2) shows, in some instances the maximum displacement is observed not on the surface of a rolled sheet but in the subsurface region. These types of curves are typically observed in FEM simulations, whereas the model parameters (B_1, B_2 and B_3) can easily be determined for each particular case by fitting procedure. Comparing Eqs. (3) and (5), it becomes obvious that the simplified deformation model (SDM) can reproduce the quasi parabolic function of Eq. (3) if $B_1=0$ and $A=B_3$. Since the material flow is controlled by the roll gap geometry and friction coefficient, it is reasonable to suggest the model parameters will also be. The SDM model use the diameter of the roll, the initial thickness, the final thickness and the friction coefficient as inputs for calculating different parameters of the model.

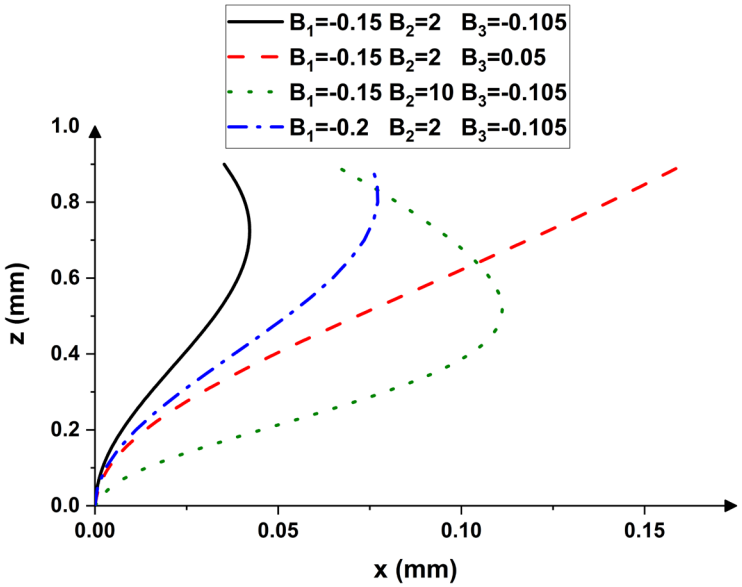

Figure 2
Distortion of initially vertical line as predicted by the extended function with specified model parameters

4 Results

Fig. (3) reveals the two ends of the deformation spectrum: A) small reduction with a small value of friction coefficient (R=250 mm, h_0=1 mm, h=0.9 mm, r=0.1, μ=0.08, v=2 m/min) and B) relatively large straining with the larger value of friction coefficient (R=250 mm, h_0=1 mm, h=0.6 mm, r=0.4, μ=0.25, v=2 m/min). In both cases, the linear velocity of rolls was identical v=2 m/min, this means, that this rolling process is a symmetric rolling. As it is shown in Fig (3a), the application of a small reduction degree with low values of μ accounts for reverse displacement and this phenomenon can be captured by the extended function (SDM, Eq. (5)), while the flow line model [7] fails to reproduce this deformation pattern. In the case of relatively large straining with larger μ, both the FLM and SDM can successfully reproduce the displacement curve calculated by FEM. It can be concluded here that the reverse displacement tends to vanish by increasing the degree of deformation.

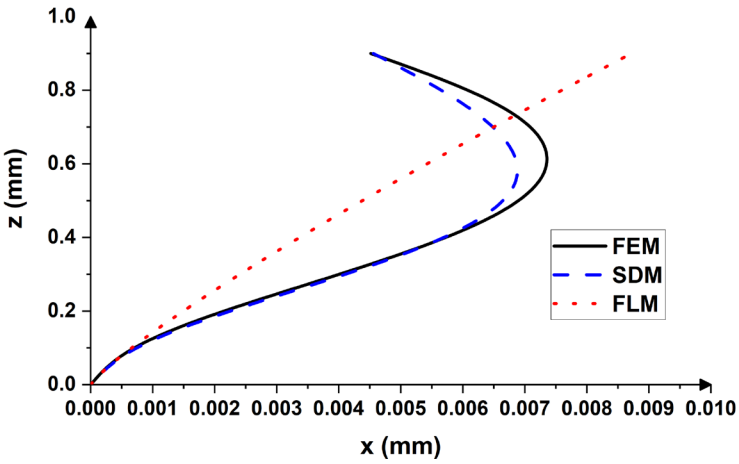

(a)

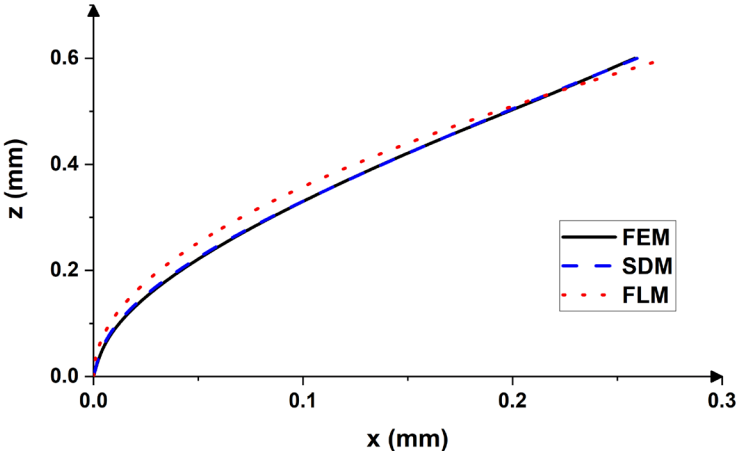

(b)

Figure 3

Displacement patterns calculated by FEM, FLM [7] and SDM for various roll gap geometries: a) R=250 mm, h_0=1 mm, h=0.9 mm, r=0.1, μ=0.08, v=2 m/min; b) R=250 mm, h_0=1 mm, h=0.6 mm, r=0.4, μ=0.25, v=2 m/min

4.1 Determining the Model Parameters

In order to make the model practically attainable, the model parameters (B_1, B_2 and B_3) of Eq. (5) should be determined. It is suggested here by Eqs. (6-8) that parameters B_1-B_3 are functions of friction coefficient μ while the polynomial coefficients p_{ij} depend on the reduction degree r. In Eq. (9), the s_{ijk} coefficients are fitting parameters.

$$B_i = p_{i3} \cdot \mu^3 + p_{i2} \cdot \mu^2 + p_{i1} \cdot \mu + p_{i0} \tag{6}$$

$$p_{ij} = s_{ij3} \cdot r^3 + s_{ij2} \cdot r^2 + s_{ij1} \cdot r + s_{ij0} \tag{7}$$

To determine the s_{ijk}, the square sum of the difference between the SDM patterns and ones calculated by FEM need to be minimalized according to Eq. (8):

$$f(\mu, r, z, \bar{\bar{s}}) = \sum_{\mu} \sum_{\bar{\bar{s}}} \left[x_{appr}(\mu, r, z) - x_{FEM} \right]^2 \tag{8}$$

The minimum can be determined by the multivariable extreme value defined in Eq. (9):

$$\frac{\partial f(\mu, r, z, \bar{\bar{s}})}{\partial \bar{\bar{s}}} = \bar{0} \tag{9}$$

Due to a large number of variables, a system of 12 equations with 12 variables was created. The solution for this equation-system was found by the Nonlinear programming method. The s_{ijk} parameters, presented in Table 1 were defined from the results presented in [6] [8] [9]. It should be underlined that the parameters of Table 1 are applicable for aluminum alloys, while the same procedure can be repeated for other metals as well.

Table 1
Parameters fitted for Eq. (5)

	s_{xx3}	s_{xx2}	s_{xx1}	s_{xx0}
s_{13x}	-4.78	315.92	-85.11	0.58
s_{12x}	-8	-381.3	154.26	-12.97
s_{11x}	-23.94	99.61	-38.84	3.35
s_{10x}	-2.58	-2.53	1.4	-0.15
s_{23x}	-0.01	237042	-131188.6	15426.6
s_{22x}	-0.21	-133149.5	71118.7	-7884.67
s_{21x}	-0.91	22114.4	-11439.6	1186.25
s_{20x}	3.94	-1009.74	514.72	-44.56
s_{33x}	6.27	5.04	0.35	-15.24
s_{32x}	19.32	-391.02	172.8	-11.45
s_{31x}	37.88	101.43	-44.28	3.67
s_{30x}	-6.36	-2.29	1.6	-0.17

Knowing the s_{ijk} values enables the calculation of deformation distribution across the thickness of rolled sheets under various conditions. Fig. (4) shows the displacement patterns of initially vertical lines calculated by FEM and approximated by the simplified mathematical model of Eq. (5) with s_{ijk} coefficients of Table 1 for various thickness reductions and diverse friction

conditions. It is evident that the mathematical model employed provides very satisfactory results since the deviations between the FEM and SDM curves are negligibly small. It is obvious that the phenomenon of reverse displacement can be neglect for rolling under relatively dry condition (higher μ).

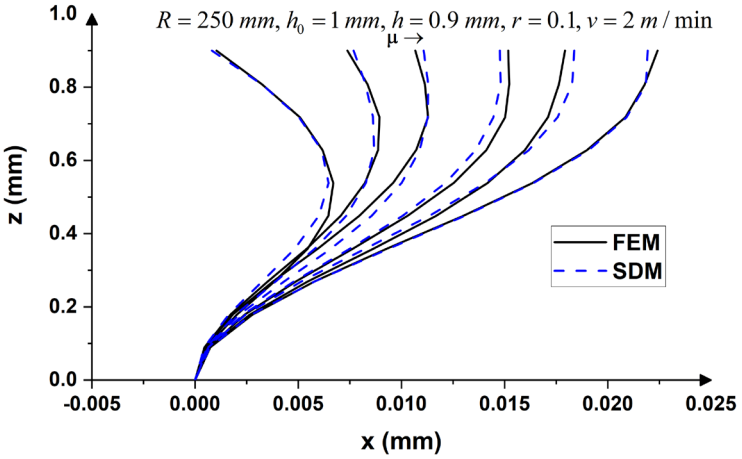

Figure 4

Displacement curves of initially vertical lines calculated by FEM (continuous line) and simplified mathematical model (Eq. (5), dashed lines) for thickness reduction R=250 mm, h_0=1 mm, h=0.9 mm, r=0.1, μ=(0.075, 0.1, 0.15, 0.175, 0.2, 0.25), v=2 m/min

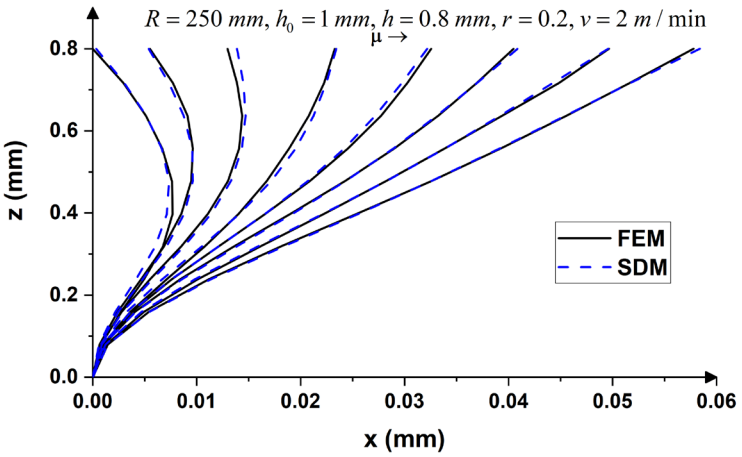

Figure 5

Displacement curves of initially vertical lines calculated by FEM (continuous line) and simplified mathematical model (Eq. (5), dashed lines) for thickness reduction R=250 mm, h_0=1 mm, h=0.8 mm, r=0.2, μ=(0.025, 0.06, 0.1375, 0.15, 0.175, 0.2, 0.225, 0.25), v=2 m/min

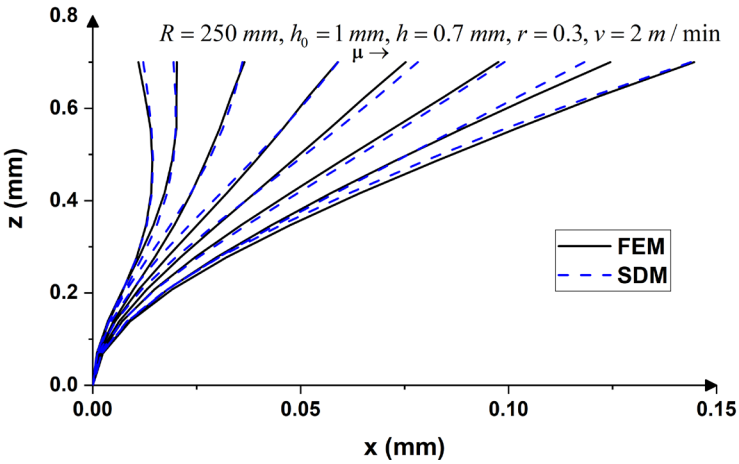

Figure 6

Displacement curves of initially vertical lines calculated by FEM (continuous line) and simplified mathematical model (Eq. (5), dashed lines) for thickness reduction R=250 mm, h_0=1 mm, h=0.7 mm, r=0.3, μ=(0.08, 0.1, 0.125, 0.15, 0.175, 0.2, 0.225, 0.25), v=2 m/min

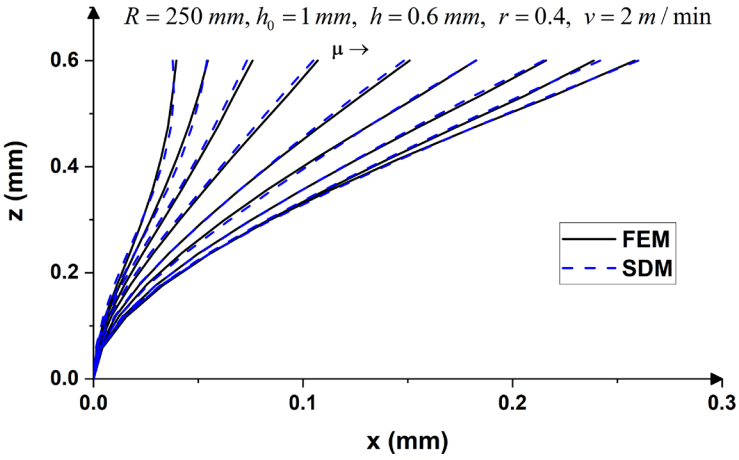

Figure 7

Displacement curves of initially vertical lines calculated by FEM (continuous line) and simplified mathematical model (Eq. (5), dashed lines) for thickness reduction R=250 mm, h_0=1 mm, h=0.6 mm, r=0.4, μ=(0.075, 0.9 0.1, 0.125, 0.15, 0.175, 0.2, 0.225, 0.25), v=2 m/min

To calculate the equivalent (von Mises) strain, it is necessary to estimate the deformation in both horizontal and vertical directions, which are typically considered uniform along the cross-section of a rolled sheet. The normal and shear components of deformation as well as the equivalent strain [13] can be computed according to Eqs. (10-13):

$$\varepsilon_{zz}(z) = -\varepsilon_{xx}(z) = -\ln\left(\frac{h_0}{h}\right) \tag{10}$$

$$\gamma_{zx}(z) = \gamma_{xz}(z) = \gamma(z) = \frac{dx(z)}{dz} = -2B_1 \cdot B_2 \cdot ze^{-B_2 z^2} + 2B_3 \cdot z \tag{11}$$

$$\varepsilon_{vM}(z) = \frac{1}{\sqrt{3}}\sqrt{4 \cdot \varepsilon_{xx}^2(z) + \gamma^2(z)} \tag{12}$$

The shear distribution across the thickness is not homogeneous (Fig. (8)) implying that the equivalent strain will also reveal heterogeneous character along the normal direction (Fig. (9)). As can be seen in Fig. (8), the shear strain is not linear in investigated cases A and B. In case of condition A, the maximum is observed in the subsurface region due to phenomenon of reverse shear, while in case of B the amount of γ first linearly increases from the mid-thickness to the sub-surface and afterward tends to saturate within the surface layers. The analytical model developed in this work is capable of reproducing the evolutionary patterns of strain evolution presented in Figs. (8) and (9). The deviations observed between the SDM and FEM are attributed to the simplifications made in the proposed model.

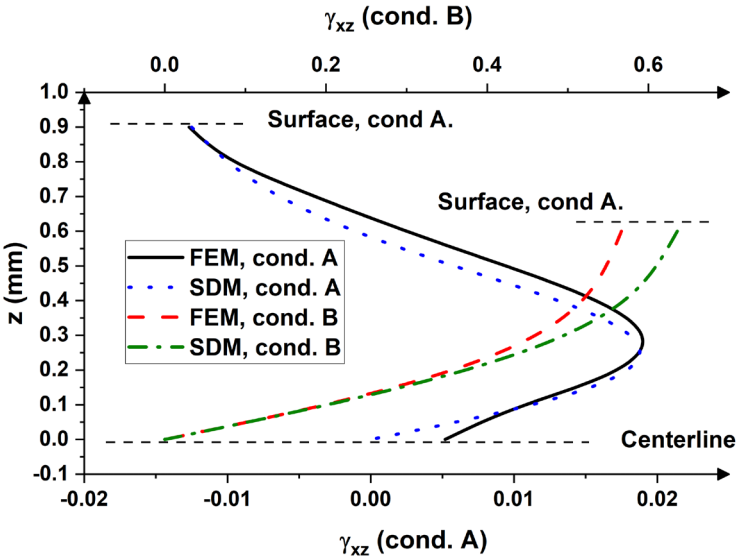

Figure 8

Distribution of shear strain for different rolling conditions as predicted by the new analytical model: a) condition A (R=250 mm, h_0=1 mm, h=0.9 mm, r=0.1, μ=0.08, v=2 m/min); b) condition B (R=250 mm, h_0=1 mm, h=0.6 mm, r=0.4, μ=0.25, v=2 m/min)

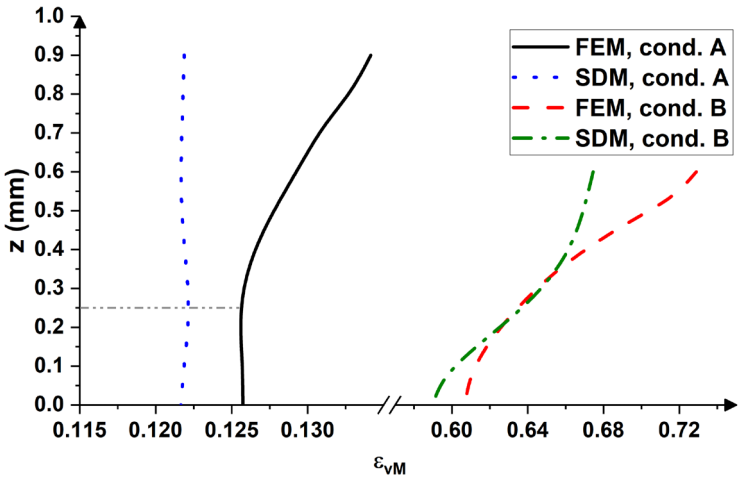

Figure 9

Distribution of von Mises strain for different rolling conditions as predicted by the new analytical model: a) condition A (R=250 mm, h_0=1 mm, h=0.9 mm, r=0.1, μ=0.08, v=2 m/min); b) condition B (R=250 mm, h_0=1 mm, h=0.6 mm, r=0.4, μ=0.25, v=2 m/min)

Alternatively, to Eqs. (10-12), the assessment of both shear and equivalent strains can be calculated by employing Eqs. (13) and (14). The accuracy of this method was tested on the ultrafine-grain structured metals [16]. Since the shear strain is mainly localized within the surface layer for a higher thickness reduction as a result of the reverse flow phenomenon, it was suggested to calculate the surface strain ε_s, while the ε_{vM} is computed by substituting Eqs. (13) and (14):

$$\varepsilon_s = \frac{2(1-r)^2}{r(2-r)}\gamma \ln\left(\frac{1}{1-r}\right) \tag{13}$$

$$\varepsilon_{vM} = \sqrt{\frac{4}{3}\left(\ln\left(\frac{1}{1-r}\right)\right)^2 + \frac{\varepsilon_s^2}{3}} \tag{14}$$

Both Eq. (14) and (12) require the amount of γ, imposed by rolling, which can be computed using Eq. (11). Fig. (10) suggests that these two methods, Eqs. (12) and (14), provide similar results.

Table 2
Shear and equivalent strain values according to different methods and calculations

Condition	Equation	FEM		FLM		SDM	
		ε_s	ε_{eq}	ε_s	ε_{eq}	ε_s	ε_{eq}
A	Eq. (12)	-0.01669	0.1159	0.01167	0.1157	-0.1149	0.1157
A	Eq. (14)	-0.1499	0.1219	0.01048	0.1218	-0.01032	0.1218
B	Eq. (12)	0.5852	0.5723	0.8675	0.6812	0.6279	0.5872
B	Eq. (14)	0.3363	0.6210	0.4985	0.6263	0.3609	0.6256

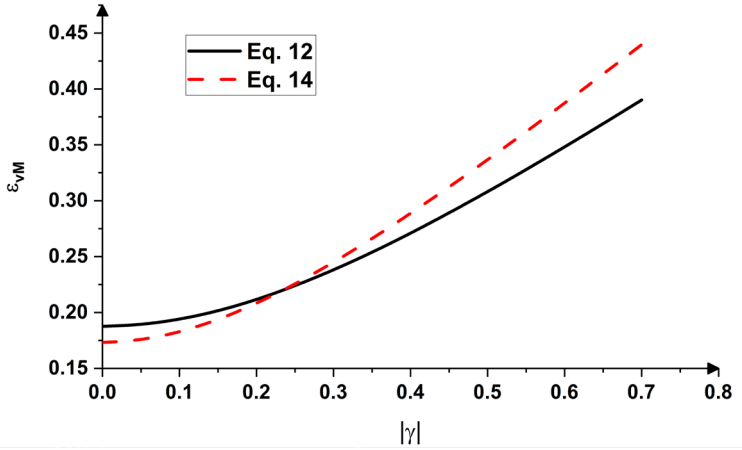

Figure 10
Measured (a) and calculated (b) displacement patterns for 30% thickness reduction (h=0.7 mm and μ=0.075). The dotted lines on graph (b) represent the upper and lower bounds of experimental variations

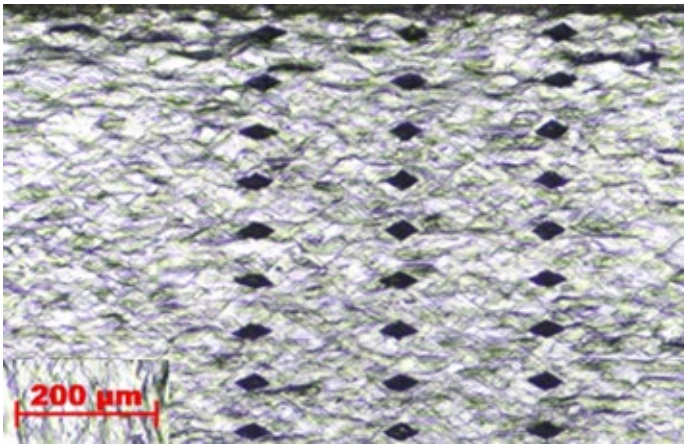

(a)

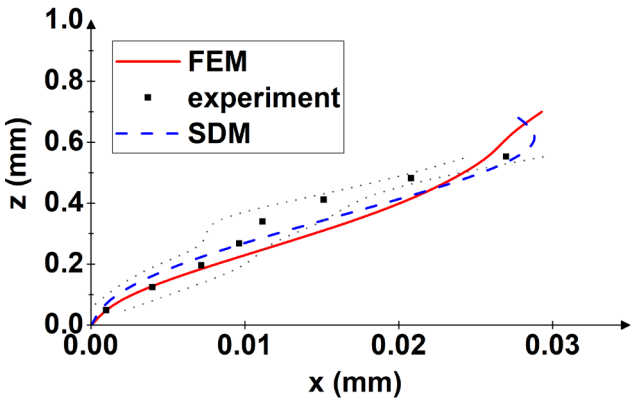

(b)

Figure 11
Displacement for R=250 mm, h_0=1 mm, h=0.7 mm, r=0.3, μ=0.075, v=2 m/min, (a) measured values, (b) data

Table 2 summarizes both shear and equivalent strain values calculated for various roll gap geometries by various equations. As it follows from Table 2, the FEM and SDM methods ensure similar values for ε_s and ε_{eq}, while the FLM is less accurate in capturing the shear strain.

Fig. (11a) presents the distortion patterns of initially vertical lines, made by microindentation, after r=30% thickness reduction in 1050 Al alloy. As it turns out (Fig. (11b)), both FEM and SDM outputs are in good agreement with the experimentally measured counterparts.

4.2 Calculation of Stress Values

Knowing the equivalent strains and material's hardening law [18], the von Mises stress distribution can be evaluated by Eq. (15). The calculated stress distribution for cases A and B reveals that stress variations across the thickness are approximately 5%. The calculated stresses for different rolling conditions as predicted by both FEM and the new analytical model for conditions A (R=250 mm, μ=0.08, h_0=1 mm, h=0.9 mm, v=2 m/min) and B (R=250 mm, μ=0.25, h_0=1 mm, h=0.6 mm, v=2 m/min) are as following: $\sigma_{vM,FEM}$ (A-surface)= 99.03 MPa, $\sigma_{vM,SDM}$ (A-surface)= 97.15 MPa, $\sigma_{vM,FEM}$ (A-mid-thickness)= 97.79 MPa, $\sigma_{vM,SDM}$ (A-mid-thickness)= 97.12 MPa, $\sigma_{vM,FEM}$ (B-surface)= 138.93 MPa, $\sigma_{vM,SDM}$ (B-surface)= 136.79 MPa, $\sigma_{vM,}$ FEM (B-mid-thickness)= 133.93 MPa, $\sigma_{vM,SDM}$ (B-mid-thickness)= 133.17 MPa. This change seems to be negligibly small, but it should be noted that even small stress diversities are capable of triggering the evolution of microstructural heterogeneities in variously oriented grains.

$$\sigma_{vM} = 148 \cdot \varepsilon_{vM}^{0.2} \left[\text{MPa}\right] \tag{15}$$

Apart from the above formulation, there are other material models, such as the cubic polynomial strain-stress function described in Ref. [14] or the Ramberg-Osgood model [19].

The presented analytical model can be employed for the estimation of the strain/stress distribution as well as the amount of shear strain/stress in cold rolled aluminum sheets or other metals. There are many pros and cons regarding the implementation of SDM. Results of experimental observations and FEM simulations clearly demonstrate that the major advantage of the analytical model developed is that it can accurately capture the evolution of both strain and stress heterogeneity across the thickness of a rolled sheet. Compared to time costly FEM simulations, this approach is capable of providing a solution within a fraction of a second. It should be noted that this model cannot predict the strain/stress evolution over time and neglects the effect of temperature and rolling velocity, however, the effect of these technological parameters on properties of cold rolled materials is negligibly small. The model can be extended by taking into account the deflection of the rolls as it is described elsewhere [20]. The disadvantage of the presented approach is that the model parameters should be defined for each roll diameter individually, though, the fitting parameters can be defined for various rolling stands according to the procedure, presented in this contribution, and this will ensure a very fast and accurate simulation of cold rolling process.

Conclusions

The normal and shear components of material strain, introduced by rolling, can be accurately modelled, by the presented analytical description. The model parameters were defined from previously published experimental data, found in various literature sources, and results of finite element calculations.

The new model reveals very reasonable agreement with the data calculated by FEM and ones measured experimentally. The approach can be used for the description of evolution of strain components in cold rolling. The presented analytical solution was successfully tested for thickness reductions ranging from 10% to 40% while the friction coefficient varied between 0.025 and 0.25. The discrepancies observed between the FEM calculations and ones produced by the analytical model developed are attributed to the simplifications made in the SDM.

Compared to finite element or flow line models, the developed approach neglects the kinetics of material flow, nonetheless, it can guarantee a high accuracy of strain evolution in cold rolling process. The extended model can be used for rapid analysis of symmetric rolling and is capable of capturing the phenomenon of reverse displacement in Al alloys. By determining corresponding model parameters, this approach can be employed for strain/stress evolution in various metals. Results of model calculations suggest that the reverse displacement tends to disappear, by increasing both the degree of deformation and friction coefficient.

Acknowledgement

Project no. TKP2021-NVA-29 has been implemented with the support provided by the Ministry of Innovation and Technology of Hungary from the National Research, Development and Innovation Fund, financed under the TKP2021-NVA funding scheme.

References

[1] Boldetti, C., Pinna, C., Howard, I. C., Guttierez, G., "Measurement of deformation gradients in hot rolling of AA3004", Experimental Mechanics, Vol. 45, pp. 517-525, 2005, DOI: 10.1007/BF02427905

[2] Roumina, R., Sinclair, C., "Deformation geometry and through-thickness strain gradients in asymmetric rolling", Metallurgical and Materials Transactions A – Physical Metallurgy and Materials Science, Vol. 39, pp. 2495-2503, 2008, DOI: 10.1007/s11661-008-9582-6

[3] Sidor, J. J., Petrov, R., Kestens, L., "Texture control in aluminium sheets by conventional and asymmetric rolling", In: Comherensive Materials Processing, Vol. 3: Advanced Forming Technologies, Elsevier, pp. 447-498, 2014, DOI: 10.1016/B978-0-08-096532-1.00324-1

[4] Beausir B., Tóth L., "A New Flow Function to Model Texture Evolution in Symmetric and Asymmetric Rolling", In: Haldar A., Suwas S., Bhattacharjee D. (eds), Microstructure and Texture in Steels, Springer, London, 2009, pp. 415-420, DOI: 10.1007/978-1-84882-454-6_25

[5] Sidor, J. J., "Deformation texture in Al alloys: Continuum mechanics and crystal plasticity aspects", Modelling and Simulation in Materials Science and Engineering, Vol. 26(8), 085011, 2018, DOI: 10.1088/1361-651X/aae886

[6] Sidor, J. J., "Assessment of flow-line model in rolling texture simulations", Metals Vol. 9(10), 1098, 2019, DOI: 10.3390/met9101098

[7] Decroos, K., Sidor, J. J., Seefeldt, M., "A new analytical approach for velocity field in rolling processes and its application in through-thickness texture prediction", Metallurgical and Materials Transactions A, Vol. 45, pp. 948-961, 2014, DOI: 10.1007/s11661-013-2021-3

[8] Sidor, J. J., Xie, Q., "Deformation texture modelling by mean-field and full-field approaches", Advanced Materials Letters, Vol. 10(9), pp. 643-650, 2019, DOI: 10.5185/amlett.2019.0030

[9] Cawthorn, C. J., Loukaides, E., Allwood, J., "Comparison of analytical models for sheet rolling", Procedia Engineering, Vol. 81, pp. 2451-2456, 2014, DOI: 10.1016/j.proeng.2014.10.349

[10] Minton, J., Cawthorn, C. J., Brambley, E., "Asymptotic analysis of asymmetric thin sheet rolling", International Journal of Mechanical Sciences, Vol. 113, pp. 36-48, 2016, DOI: 10.1016/j.ijmecsci.2016.03.024

[11] Avitzur, B., "Friction-aided strip rolling with unlimited reduction", International Journal of Machine Tool Design and Research, Vol. 20(3-4), pp. 197-210, 1980, DOI: 10.1016/0020-7357(80)90004-9

[12] Szűcs, M., "Többszintű modellezés alkalmazása a szimmetrikus és az aszimmetrikus hengerlési folyamatok vizsgálatára" (The use of multi-scale modelling to study symmetric and asymmetric rolling processes), PHD Thesis, University of Miskolc, Hungary, 2017 (in Hungarian) [online] Available at: http://193.6.1.94:9080/JaDoX_Portlets/documents/document_25524_section_20959.pdf [Accessed: 25 09 2021]

[13] Pesin, A., Pustovoytov, D., "Influence of process parameters on distribution of shear strain through sheet thickness in asymmetric rolling", Key Engineering Materials, Vol. 622-623, pp. 925-935, 2014, DOI: 10.4028/www.scientific.net/KEM.622-623.929

[14] Ďurovský, F., Zboray, L., Ferková, Ž., "Computation of rolling stand parameters by genetic algorithm", Acta Polytechnica Hingarica, Vol. 5, No. 2, pp. 59-70, 2008

[15] Inoue, T., "Strain variations on rolling condition in accumulative roll-bonding by finite element analysis", In: David Moratal (ed.), Finite Element Analysis, InTech, London pp. 598-610, 2010, DOI: 10.5772/10233

[16] Ma, C., Hou, L., Zhang, J., Zhuang, L., "Experimental and numerical investigation of plastic deformation during multi-pass asymmetric and symmetric rolling of high-strength aluminium alloys", Material Science Forum, Vol. 794-796, pp. 1157-1162, 2014, DOI: 10.4028/www.scientific.net/MSF.794-796.1157

[17] Inoue, T., Qiu, H., Ueji, R., "Though-thickness microstructure and strain distribution in steel sheets rolled in a large-diameter rolling process", Metals, Vol. 10(1) 91, 2020, DOI: 10.3390/met10010091

[18] Van Haaften, V. M., Magnin, B., Kool, W. H., Katgerman, L., "Constitutive behavior of as-cast AA1050, AA3104, and AA5182", Metallurgical and Materials Transactions A, Vol. 33A, pp. 1971-1980, 2002, DOI: 10.1007/s11661-002-0030-8

[19] Ziha, K., "Stress-strain interaction model of plasticity", Acta Polytechnica Hungarica, Vol. 12, No. 1, pp. 41-54, 2015, DOI: 10.12700/APH.12.1.2015.1.3

[20] Kucsera, P., Béres, Zs., "Hot roling mill hiydraulical gap control (HGC) thickness control improvement", Acta Polytechnica Hungarica, Vol. 12, No. 6, pp. 93-106, 2015, DOI: 10.12700/aph.12.6.2015.6.6